Inorg. Chem. **2002**, *41*, 5126–5132

Mixed-Metal Uranium(VI) Iodates: Hydrothermal Syntheses, Structures, and Reactivity of $Rb[UO_2(CrO_4)(IO_3)(H_2O)]$, $A_2[UO_2(CrO_4)(IO_3)_2]$ (A = K, Rb, Cs), and $K_2[UO_2(MoO_4)(IO_3)_2]$

Richard E. Sykora, Steven M. McDaniel, Daniel M. Wells, and Thomas E. Albrecht-Schmitt*

Department of Chemistry, Auburn University, Auburn, Alabama 36849

Received June 5, 2002

The reactions of the molecular transition metal iodates $A[CrO_3(IO_3)]$ (A = K, Rb, Cs) with UO_3 under mild hydrothermal conditions provide access to four new, one-dimensional, uranyl chromatoiodates, $Rb[UO_2(CrO_4)(IO_3)(H_2O)]$ (**1**) and $A_2[UO_2(CrO_4)(IO_3)_2]$ (A = K (**2**), Rb (**3**), Cs (**4**)). Under basic conditions, MoO_3, UO_3, and KIO_4 can be reacted to form $K_2[UO_2(MoO_4)(IO_3)_2]$ (**5**), which is isostructural with **2** and **3**. The structure of **1** consists of one-dimensional $^1_\infty[UO_2(CrO_4)(IO_3)(H_2O)]^-$ ribbons that contain uranyl moieties bound by bridging chromate and iodate anions as well as a terminal water molecule to create $[UO_7]$ pentagonal bipyramidal environments around the U(VI) centers. These ribbons are separated from one another by Rb^+ cations. When the iodate content is increased in the hydrothermal reactions, the terminal water molecule is replaced by a monodentate iodate anion to yield **2**–**4**. These ribbons can be further modified by replacing tetrahedral chromate anions with MoO_4^{2-} anions to yield isostructural, one-dimensional $^1_\infty[UO_2(MoO_4)(IO_3)_2]^{2-}$ ribbons. Crystallographic data: **1**, triclinic, space group $P\bar{1}$, a = 7.3133(5) Å, b = 8.0561(6) Å, c = 8.4870(6) Å, α = 88.740(1)°, β = 87.075(1)°, γ = 71.672(1)°, Z = 2; **2**, monoclinic, space group $P2_1/c$, a = 11.1337(5) Å, b = 7.2884(4) Å, c = 15.5661(7) Å, β = 107.977(1)°, Z = 4; **3**, monoclinic, space group $P2_1/c$, a = 11.3463(6) Å, b = 7.3263(4) Å, c = 15.9332(8) Å, β = 108.173(1)°, Z = 4; **4**, monoclinic, space group $P2_1/n$, a = 7.3929(5) Å, b = 8.1346(6) Å, c = 22.126(2) Å, β = 90.647(1)°, Z = 4; **5**, monoclinic, space group $P2_1/c$, a = 11.3717(6) Å, b = 7.2903(4) Å, c = 15.7122(8) Å, β = 108.167(1)°, Z = 4.

Introduction

Nature has provided us with glimpses of the unusual nature of U(VI) compounds that contain oxoanions with nonbonding electrons in the form of uranyl selenites and tellurites. These minerals include derriksite, $Cu_4[(UO_2)(SeO_3)_2](OH)_6$,[1] demesmaekerite, $Pb_2Cu_5[(UO_2)(SeO_3)_3]_2(OH)_6(H_2O)_2$,[2] guilleminite, $Ba[(UO_2)_3(SeO_3)_2O_2](H_2O)_3$,[3] marthozite, $Cu[(UO_2)_3(SeO_3)_2O_2](H_2O)_8$,[4] cliffordite, $UO_2(Te_3O_7)$,[5] moctezumite, $PbUO_2(TeO_3)_2$,[6] and schmitterite, $UO_2(TeO_3)$.[7] As can be seen from this list, this group is quite small, necessitating synthetic studies to expand our understanding of the nature of bonding in these compounds. One of the driving forces behind this work is to understand the effects of the stereochemically active lone pair of electrons on the Se(IV) and Te(IV) centers and the overall crystal structure. The general tendency is for nonbonding electrons to reduce the dimensionality of crystalline solids[8−13] and to create noncentrosymmetric structures owing to the alignment of these lone pairs.[14−29] This trend has held true in uranyl selenites, where

* Author to whom correspondence should be addressed. E-mail: albreth@auburn.edu.

(1) Ginderow, D.; Cesbron, F. *Acta Crystallogr*. **1983**, *C39*, 1605.
(2) Ginderow, D.; Cesbron, F. *Acta Crystallogr*. **1983**, *C39*, 824.
(3) Cooper, M. A.; Hawthorne, F. C. *Can. Mineral*. **1995**, *33*, 1103.
(4) Cooper, M. A.; Hawthorne, F. C. *Can. Mineral.* **2001**, *39*, 797.
(5) Branstätter, F. *TMPM, Tschermaks Mineral. Petrogr. Mitt*. **1981**, *29*, 1.
(6) Swihart, G. H.; Gupta, P. K. S.; Schlemper, E. O.; Back, M. E.; Gaines, R. V. *Am. Mineral*. **1993**, *78*, 835.
(7) Meunier, G.; Galy, J. *Acta Crystallogr*. **1973**, *B29*, 1251.
(8) Bean, Amanda C.; Peper, Shane M.; Albrecht-Schmitt, T. E. *Chem. Mater*. **2001**, *13*, 1266.
(9) Meschede, W.; Mattes, R. *Z. Anorg. Allg. Chem.* **1976**, *420*, 25.
(10) Sykora, R. E.; Wells, D. M.; Albrecht-Schmitt, T. E. *J. Solid State Chem.* **2002**, *166*, 442.
(11) Bean, A. C.; Ruf, M.; Albrecht-Schmitt, T. E. *Inorg. Chem*. **2001**, *40*, 3959.
(12) Mistryukov, V. E.; Michailov, Y. N. *Koord. Khim*. **1983**, *9*, 97.
(13) Harrison, W. T. A.; Dussack, L. L.; Jacobson, A. J. *J. Solid State Chem.* **1996**, *125*, 234.
(14) Bergman, J. G., Jr.; Boyd, G. D.; Ashkin, A.; Kurtz, S. K. *J. Appl. Phys.* **1969**, *70*, 2860.
(15) Sykora, R. E.; Ok, K. M.; Halasyamani, P. S.; Albrecht-Schmitt, T. E. *J. Am. Chem. Soc*. **2002**, *124*, 1951.

10.1021/ic025773y CCC: $22.00
Published on Web 09/11/2002

all representatives contain one- or two-dimensional frameworks.[1−4,30−32] However, uranyl tellurites defy this empiricism and form one-, two-, and three-dimensional structures.[5−7,33−35]

In order to address the crystal chemistry and properties of U(VI) compounds containing oxoanions with stereochemically active lone pairs electrons, we have been preparing a family of uranyl iodates containing different classes of countercations. These compounds are represented by $A_2[(UO_2)_3(IO_3)_4O_2]$ (A = K, Rb, Tl),[11,36] $Cs_2[(UO_2)_3Cl_2(IO_3)(OH)O_2]\cdot 2H_2O$,[37] $AE[(UO_2)_2(IO_3)_2O_2](H_2O)$ (AE = Sr, Ba, Pb),[11,36] and $Ag_4(UO_2)_4(IO_3)_2(IO_4)_2O_2$.[38] The structures of these uranyl iodates are one- or two-dimensional as expected. However, there are substantial differences in the U(VI) coordination environments, in the binding modes of the iodate anions, and even in the oxoanion species themselves. For example, UO_6 tetragonal bipyramids, UO_7 pentagonal bipyramids, and UO_8 hexagonal bipyramids have all been identified in these structures.

One of the features lacking in these compounds is the presence of redox-active metal centers. In order to address this vacancy we are experimenting with the use of molecular transition metal iodate starting materials, such as the chromyliodate anion, $[CrO_3(IO_3)]^-$, as sources of both transition metals and iodate anions. These initial studies resulted in a preliminary communication on the synthesis and structure of $Cs_2[UO_2(CrO_4)(IO_3)_2]$.[39] In this report we substantially expand on our early work with details on the new one-dimensional uranyl chromatoiodates, $Rb[UO_2(CrO_4)(IO_3)(H_2O)]$ (**1**) and $A_2[UO_2(CrO_4)(IO_3)_2]$ (A = K (**2**), Rb (**3**), Cs (**4**)), and the molybdate analogue of these compounds, $K_2[UO_2(MoO_4)(IO_3)_2]$ (**5**).

Experimental Section

Syntheses. UO_3 (99.8%, Alfa-Aesar), CsCl (99.9%, Alfa-Aesar), RbCl (99%, Alfa-Aesar), KCl (Ultrapure, Alfa-Aesar), I_2O_5 (98%, Alfa-Aesar), Cs_2CO_3 (99%, Alfa-Aesar), Rb_2CO_3 (99%, Alfa-Aesar), H_5IO_6 (98%, Alfa-Aesar), HIO_3 (99.5%, Alfa-Aesar), $K_2Cr_2O_7$ (ACS certified, Fisher), CrO_3 (99.8%, J. T. Baker), and MoO_3 (99.95%, Alfa-Aesar) were used as received. AIO_4 (A = Rb, Cs)[40] and $K[CrO_3(IO_3)]$[41] were prepared by literature methods. $Rb[CrO_3(IO_3)]$ and $Cs[CrO_3(IO_3)]$ were prepared by heating an equimolar amount of the appropriate alkali metal metaperiodate with CrO_3 in aqueous media at 180 °C for 72 h. Distilled and Millipore filtered water with a resistance of 18.2 MΩ was used in all reactions. Reactions were run in Parr 4749 23 mL autoclaves with PTFE liners. The reactions reported produced the highest yields of the desired compounds. SEM/EDX analyses were performed using a JEOL 840/Link Isis instrument. U, Cr, Mo, and K percentages were calibrated against standards. Typical results are within 3% of actual ratios. IR spectra were collected on a Nicolet 5PC FT-IR spectrometer from KBr pellets. ***WARNING:*** *While the UO_3 contains depleted U, standard precautions for handling radioactive materials should be followed. Old sources of depleted U should not be used, as the daughter elements of natural decay are highly radioactive and present serious health risks.*

$Rb[UO_2(CrO_4)(IO_3)(H_2O)]$ (1). UO_3 (216 mg, 0.75 mmol), CrO_3 (75 mg, 0.75 mmol), and $RbIO_4$ (209 mg, 0.75 mmol) were loaded into an autoclave. Water (0.5 mL) was then added to the solids. The autoclave was heated at 180 °C for 72 h and slow cooled at 9 °C/h to 22 °C. The product consisted of yellow needles of **1** with no liquid remaining in the autoclave. Yield for **1**: 491 mg (98% based on U). EDX analysis provided a Rb:U:Cr:I ratio of 1:1:1:1. IR (KBr, cm^{-1}):[42,43] 3262 (ν_{OH}, s, br), 1624 (δ_{OH}, m), 956 (ν_{CrO}, s), 943 (ν_{CrO}, s), 914 ($\nu_{3[uranyl]}$, s), 874 (ν_{CrO}, s), 834 ($\nu_{1[uranyl]}$, s), 803 (ν_{IO}, s), 783 (ν_{IO}, s), 733 (ν_{IO}, s, sh), 722 (ν_{IO}, s, sh), 671 (ν_{IO}, m, sh).

$K_2[UO_2(CrO_4)(IO_3)_2]$ (2). UO_3 (156 mg, 0.55 mmol) and $K[CrO_3(IO_3)]$ (344 mg, 1.10 mmol) were loaded into an autoclave. Water (0.5 mL) was then added to the solids. The autoclave was heated at 180 °C for 86 h and slow cooled at 9 °C/h to 22 °C. The products consisted of orange prisms of $K_2Cr_2O_7$ and golden rods of **2** with no remaining liquid. Yield for **2**: 310 mg (70% based on U). EDX analysis provided a K:U:Cr:I ratio of 2:1:1:2. IR (KBr, cm^{-1}):[42,43] 956 (ν_{CrO}, s), 943 (ν_{CrO}, s), 902 ($\nu_{3[uranyl]}$, m), 873 (ν_{CrO}, s), 831 ($\nu_{1[uranyl]}$, m), 815 (ν_{IO}, s), 798 (ν_{IO}, m), 775 (ν_{IO}, s), 742 (ν_{IO}, s), 730 (ν_{IO}, s), 699 (ν_{IO}, s, br).

$Rb_2[UO_2(CrO_4)(IO_3)_2]$ (3). UO_3 (221 mg, 0.77 mmol) and $Rb[CrO_3(IO_3)]$ (279 mg, 0.77 mmol) were loaded into an autoclave. Water (0.5 mL) was then added to the solids. The autoclave was

(16) Sykora, R. E.; Ok, K. M.; Halasyamani, P. S.; Wells, D. M.; Albrecht-Schmitt, T. E. *Chem. Mater.* **2002**, *14*, 2741.
(17) Kwon, Y.-U.; Lee, K.-S.; Kim, Y. H. *Inorg. Chem.* **1996**, *35*, 1161.
(18) Vaughey, J. T.; Harrison, W. T. A.; Dussack, L. L.; Jacobson, A. J. *Inorg. Chem.* **1994**, *33*, 4370.
(19) Svenson, C.; Abrahams, S. C.; Bernstein, J. L. *J. Solid State Chem.* **1981**, *36*, 195.
(20) Nassau, K.; Shiever, J. W.; Prescott, B. E.; Cooper, A. S. *J. Solid State Chem.* **1974**, *11*, 314.
(21) Liminga, R.; Abrahams, S. C.; Bernstein, J. L. *J. Chem. Phys.* **1975**, *62*, 755.
(22) Abrahams, S. C.; Bernstein, J. L.; Nassau, K. *J. Solid State Chem.* **1976**, *16*, 173.
(23) Liminga, R.; Abrahams, S. C.; Bernstein, J. L. *J. Chem. Phys.* **1977**, *67*, 1015.
(24) Gupta, P. K. S.; Ammon, H. L.; Abrahams, S. C. *Acta Crystallogr.* **1989**, *C45*, 175.
(25) Harrison, W. T. A.; Dussack, L. L.; Jacobson, A. J. *Inorg. Chem.* **1994**, *33*, 6043.
(26) Dussack, L. L.; Harrison, W. T. A.; Jacobson, A. J. *Mater. Res. Bull.* **1996**, *31*, 249.
(27) Porter, Y.; Ok, K. M.; Bhuvanesh, N. S. P.; Halasyamani, P. S. *Chem. Mater.* **2001**, *13*, 1910.
(28) Ok, K. M.; Bhuvanesh, N. S. P.; Halasyamani, P. S. *Inorg. Chem.* **2001**, *40*, 1978.
(29) Sykora, R. E.; Wells, D. M.; Albrecht-Schmitt, T. E. *Inorg. Chem.* **2002**, *41*, 2697.
(30) Almond, P. M.; Albrecht-Schmitt, T. E. *Inorg. Chem.* **2002**, *41*, 1177.
(31) Almond, P. M.; Peper, S. M.; Bakker, E.; Albrecht-Schmitt, T. E. *J. Solid State Chem.*, in press.
(32) Loopstra, B. O.; Brandenburg, N. P. *Acta Crystallogr.* **1978**, *B34*, 1335.
(33) Burns, P. C.; Miller, M. L.; Ewing, R. C. *Can. Mineral.* **1996**, *34*, 845.
(34) Branstätter, F. *Z. Kristallogr.* **1981**, *155*, 193.
(35) Almond, P. M.; McKee, M. L.; Albrecht-Schmitt, T. E. *Angew. Chem., Int. Ed.*, in press.
(36) Bean, A. C.; Albrecht-Schmitt, T. E. *J. Solid State Chem.* **2001**, *161*, 416.
(37) Bean, A. C.; Xu, Y.; Danis, J. A.; Albrecht-Schmitt, T. E.; Runde, W. *Inorg. Chem.*, in press.
(38) Bean, A. C.; Campana, C. F.; Kwon, O.; Albrecht-Schmitt, T. E. *J. Am. Chem. Soc.* **2001**, *123*, 8806.
(39) Sykora, R. E.; Wells, D. M.; Albrecht-Schmitt, T. E. *Inorg. Chem.* **2002**, *41*, 2304.
(40) de Waal, D.; Range, K.-J. *Z. Naturforsch.* **1996**, *51b*, 1365.
(41) Loefgren, P. *Acta Chem. Scand.* **1967**, *21*, 2781.
(42) (a) Pracht, G.; Lange, N.; Lutz, H. D. *Thermochim. Acta* **1997**, *293*, 13. (b) Pracht, G.; Nagel, R.; Suchanek, E.; Lange, N.; Lutz, H. D. *Z. Anorg. Allg. Chem.* **1998**, *624*, 1355. (c) Schellenschläger, Pracht, G.; Lutz, H. D. *J. Raman Spectrosc.* **2001**, *32*, 373. (d) Peter, S.; Pracht, G.; Lange, N.; Lutz, H. D. *Z. Anorg. Allg. Chem.* **2000**, *626*, 208.
(43) (a) Nakamoto, K. *Infrared and Raman Spectra of Inorganic and Coordination Compounds*, 5th ed.; Wiley-Interscience: New York, 1997. (b) Barlett, J. R.; Cooney, R. P. *J. Mol. Struct.* **1989**, *193*, 295.

Table 1. Crystallographic Data for $Rb[UO_2(CrO_4)(IO_3)(H_2O)]$ (**1**), $K_2[UO_2(CrO_4)(IO_3)_2]$ (**2**), $Rb_2[UO_2(CrO_4)(IO_3)_2]$ (**3**), $Cs_2[UO_2(CrO_4)(IO_3)_2]$ (**4**), and $K_2[UO_2(MoO_4)(IO_3)_2$ (**5**)

	1	2	3	4	5
formula mass	664.42	814.03	906.77	1001.65	857.97
space group	$P\bar{1}$ (No. 2)	$P2_1/c$ (No. 14)	$P2_1/c$ (No. 14)	$P2_1/n$ (No. 14)	$P2_1/c$ (No. 14)
a, Å	7.255(2)	11.1337(5)	11.3463(6)	7.3929(5)	11.3717(6)
b, Å	7.990(2)	7.2884(4)	7.3263(4)	8.1346(6)	7.2903(4)
c, Å	8.418(2)	15.5661(7)	15.9332(8)	22.126(2)	15.7122(8)
α (deg)	88.738(5)	90	90	90	90
β (deg)	87.114(5)	107.977(1)	108.173(1)	90.647(1)	108.167(1)
γ (deg)	71.614(5)	90	90	90	90
V (Å^3)	462.5(2)	1201.5(1)	1258.4(1)	1330.5(2)	1237.7(1)
Z	2	4	4	4	4
T (°C)	−80	−80	−80	−80	−80
λ (Å)	0.71073	0.71073	0.71073	0.71073	0.71073
ρ_{calcd} (g cm^{-3})	4.771	4.500	4.786	5.000	4.604
μ(Mo Ka) (cm^{-1})	265.96	202.52	263.60	230.55	197.95
$R(F)^a$	0.0319	0.0309	0.0242	0.0254	0.0169
$R_w(F_o^2)^b$	0.0906	0.0832	0.0612	0.0618	0.0397

^{a} $R(F) = \sum||F_o| - |F_c||/\sum|F_o|$. ^{b} $R_w(F_o^2) = [\sum[w(F_o^2 - F_c^2)^2]/\sum wF_o^4]^{1/2}$.

heated at 180 °C for 88.5 h and slow cooled at 9 °C/h to 22 °C. The products consisted of golden needles of **3** and yellow needles of **1**. Yield for **3**: 24 mg (7% based on I). EDX analysis provided a Rb:U:Cr:I ratio of 2:1:1:2. IR (KBr, cm^{-1}):[42,43] 955 (ν_{CrO}, s), 944 (ν_{CrO}, s), 903 ($\nu_{3[uranyl]}$, m), 875 (ν_{CrO}, m), 833 ($\nu_{1[uranyl]}$, m), 823 (ν_{IO}, w, sh), 809 (ν_{IO}, m), 801 (ν_{IO}, m, sh), 794 (ν_{IO}, w), 777 (ν_{IO}, m, br), 715 (ν_{IO}, s, br).

$Cs_2[UO_2(CrO_4)(IO_3)_2]$ (4). $Cs[CrO_3(IO_3)]$ (196 mg, 0.482 mmol), CsCl (81 mg, 0.482 mmol), UO_3 (138 mg, 0.482 mmol), and HIO_3 (85 mg, 0.482 mmol) were loaded into an autoclave. Water (0.5 mL) was then added to the solids. The autoclave was heated at 180 °C for 16 h and slow cooled at 9 °C/h to 22 °C. The products consisted of pale yellow crystals of $UO_2(IO_3)_2(H_2O)$, deep orange tablets of $Cs_2[(UO_2)_2(CrO_4)_3]$, and golden prisms of **4** with no liquid remaining in the autoclave. Yield for **4**: 300 mg (62% based on U). EDX analysis provided a Cs:U:Cr:I ratio of 2:1:1:2. IR (KBr, cm^{-1}):[42,43] 957 (ν_{CrO}, s), 944 (ν_{CrO}, s), 939 (ν_{CrO}, s, sh), 880 (ν_{CrO} or $\nu_{3[uranyl]}$, s), 870 (ν_{CrO}, s, sh), 822 ($\nu_{1[uranyl]}$, m, sh), 814 (ν_{IO}, m), 810 (ν_{IO}, m, sh), 797 (ν_{IO}, w, sh), 784 (ν_{IO}, s), 780 (ν_{IO}, s, sh), 772 (ν_{IO}, s), 727 (ν_{IO}, m, sh), 717 (ν_{IO}, s, sh), 702 (ν_{IO}, s, br). There is obvious splitting of the chromate and perhaps iodate modes in this spectrum.

$K_2[UO_2(MoO_4)(IO_3)_2]$ (5). UO_3 (217 mg, 0.76 mmol), MoO_3 (109 mg, 0.76 mmol), and KIO_4 (174 mg, 0.76 mmol) were loaded into an autoclave. Then 0.5 mL of 1.7 M KOH solution was added to the solids. The autoclave was heated at 180 °C for 136 h and slow cooled at 9 °C/h to 22 °C. Yellow rods of **5** were obtained along with an unidentified yellow polycrystalline powder. EDX determined that the powder contained K, U, and Mo. Yield for **5**: 140 mg (43% based on I). EDX analysis provided a K:U:Mo:I ratio of 2:1:1:2. IR (KBr, cm^{-1}):[42,43] 942 (ν_{MoO}, s), 917 (ν_{MoO}, s), 909 ($\nu_{3[uranyl]}$, s, sh), 893 (ν_{MoO}, s), 867 (ν_{UO}, m), 823 ($\nu_{1[uranyl]}$, s, sh), 818 (ν_{IO}, s), 811 (ν_{IO}, s, sh), 786 (ν_{IO}, s), 762 (ν_{IO}, m), 743 (ν_{IO}, s, sh), 733 (ν_{IO}, s), 703 (ν_{IO}, s, br).

Crystallographic Studies. Single crystals of $Rb[UO_2(CrO_4)(IO_3)(H_2O)]$ (**1**), $K_2[UO_2(CrO_4)(IO_3)_2]$ (**2**), $Rb_2[UO_2(CrO_4)(IO_3)_2]$ (**3**), $Cs_2[UO_2(CrO_4)(IO_3)_2]$ (**4**), and $K_2[UO_2(MoO_4)(IO_3)_2]$ (**5**) were selected for X-ray diffraction studies. The sizes for the isolated crystals were 0.250 × 0.030 × 0.024 mm for **1**, 0.126 × 0.042 × 0.032 mm for **2**, 0.305 × 0.042 × 0.038 mm for **3**, 0.260 × 0.091 × 0.053 mm for **4**, and 0.380 × 0.030 × 0.022 mm for **5**. The crystals were mounted on glass fibers with epoxy and aligned on a Bruker SMART APEX CCD X-ray diffractometer. Intensity measurements were performed using graphite-monochromated Mo Kα radiation from a sealed tube with a monocapillary collimator. SMART was used for preliminary determination of the cell constants and data collection control. For all compounds, the intensities of reflections of a sphere were collected by a combination of 3 sets of exposures (frames). Each set had a different ϕ angle for the crystal, and each exposure covered a range of 0.3° in ω. A total of 1800 frames were collected with an exposure time per frame of 30 s for compounds **1**−**5**.

For **1**−**5**, determination of integral intensities and global cell refinement were performed with the Bruker SAINT (v 6.02) software package using a narrow-frame integration algorithm. Analytical absorption corrections were applied followed by a semiempirical absorption correction using SADABS[44] with a μt parameter of 0.[30,45] The ratios of the transmission factors from the SADABS corrections were 0.702, 0.770, 0.790, 0.653, and 0.871 for **1**−**5**, respectively. The program suite SHELXTL (v 5.1) was used for space group determination (XPREP), structure solution (XS), and refinement (XL).[46] The final refinements for **1**−**5** included anisotropic displacement parameters for all atoms except O(8) in **2**, which was refined isotropically, and a secondary extinction parameter was applied to each refinement. The largest peaks and holes in the electron density maps were as follows: 2.258 and −2.875 for **1**, 1.250 and −1.309 for **2**, 2.405 and −1.332 for **3**, 1.638 and −2.148 for **4**, 0.668 and −0.933 for **5**. The largest residual electron density was always within close proximity to the heavy atoms in the structures. Some crystallographic details are listed in Table 1 for **1**−**5**; additional details can be found in the Supporting Information.

Thermal Analysis. Thermal data for $Rb[UO_2(CrO_4)(IO_3)(H_2O)]$ was collected using a TA Instruments, model 2920 differential scanning calorimeter (DSC). The sample (∼10 mg) was encapsulated in an aluminum pan and heated at 5 °C/min from 25 to 400 °C under a nitrogen atmosphere.

Results and Discussion

Syntheses. The reaction of $RbIO_4$, UO_3, and CrO_3 in a 1:1:1 ratio under mild hydrothermal conditions results in the

(44) *SADABS*. Program for absorption correction using SMART CCD based on the method of Blessing: Blessing, R. H. *Acta Crystallogr.* **1995**, *A51*, 33.
(45) Huang, F. Q.; Ibers, J. A. *Inorg. Chem.* **2001**, *40*, 2602.
(46) Sheldrick, G. M. *SHELXTL PC, Version 5.0, An Integrated System for Solving, Refining, and Displaying Crystal Structures from Diffraction Data*; Siemens Analytical X-Ray Instruments, Inc.: Madison, WI, 1994.

formation of $Rb[UO_2(CrO_4)(IO_3)(H_2O)]$ (**1**) in nearly quantitative yield. The metaperiodate anion in $RbIO_4$ is reduced in this reaction to iodate.[8,15,38,47] By using this starting material, halide ions are not introduced into the reactions to compete with iodate or chromate anions for complexation of the uranyl cations. When the iodate concentration is increased, approximately 7% of **1** is converted to $Rb_2[UO_2(CrO_4)(IO_3)_2]$ (**3**). This reaction occurs through the displacement of the water molecule in **1** by IO_3^-. However, the preparation of $K_2[UO_2(CrO_4)(IO_3)_2]$ (**2**) and $Cs_2[UO_2(CrO_4)(IO_3)_2]$ (**4**) is best accomplished by reacting UO_3 with $A[CrO_3(IO_3)]$ (A = K, Rb, Cs) in aqueous media at 180 °C.

In efforts to identify byproducts and to improve yields and purity, we have investigated the effects of stoichiometry, temperature, reaction duration, water content, and also alternative reactants on product composition and yield, and reported the highest yield syntheses in the Experimental Section. The most notable effect of alterations in reaction conditions is that crystals of these compounds are not isolated with water contents greater than 0.5 mL. In addition, variations in reaction durations have shown that while the highest yield of **2** was achieved with an 86 h reaction duration, a 16 h reaction produced the greatest yield of **4**. However, the production of **2** was not observed after 16 h. Reactions of KCl, UO_3, CrO_3, and HIO_3 have also been studied, and only trace amounts of **2** are produced by these reactions. In contrast to the preparation of **1** and **2**, the synthesis of $Cs_2[UO_2(CrO_4)(IO_3)_2]$ (**4**) is much more variable. The reaction of UO_3 with $Cs[CrO_3IO_3]$ results in the formation of **4**, with little variation in product yield upon alterations of temperature, reaction time, stoichiometry, and water content. In addition, direct reactions of CsCl, UO_3, CrO_3, and HIO_3 or CsCl, UO_3, CrO_3, and I_2O_5 result in the formation of **4**. The substitution of the CrO_4^{2-} anion by the molybdate anion, MoO_4^{2-}, is accomplished by replacing the chromyliodate anion with MoO_3 and iodate. Under basic conditions these components and KOH react to form $K_2[UO_2(MoO_4)(IO_3)_2]$ (**5**).

$UO_2(IO_3)_2(H_2O)$ is a ubiquitous byproduct in many reactions involving uranium and iodate such as those discussed above. Also, $Cs_2[(UO_2)_2(CrO_4)_3]$,[48] a new layered compound, has been isolated in the process of preparing **4**. In addition, alkali metal chromates, alkali metal dichromates, alkali metal chromyliodates, and even the new molecular compound $Cs_3(Cr_2O_7)(CrO_3IO_3)$ have all been isolated as crystalline products. All of these factors lead to the reduction of product yield in these syntheses.

Structures. $Rb[UO_2(CrO_4)(IO_3)(H_2O)]$ (1). The structure of **1** contains $[UO_7]$ pentagonal bipyramids, bridging $[CrO_4]$ tetrahedra, and bridging iodate anions that combine to form one-dimensional $^1_\infty[UO_2(CrO_4)(IO_3)(H_2O)]^-$ ribbons that propagate along the *a*-axis, as shown in Figure 1. The Rb^+ cations separate the ribbons from one another and also serve to balance charge. Dissecting the ribbons into simpler structural units leads to a more thorough understanding of the structural chemistry involved. First, each uranyl, UO_2^{2+}, moiety is bound by two chromate and two iodate anions. Two uranyl units are connected by two bridging chromate anions to form eight-membered rings. Each ring then connects with an additional ring through two bridging iodate groups. The seven-coordinate environment of each U(VI) atom is completed by a water molecule that serves to terminate the edges of the ribbon. While it is uncommon to observe water bound directly to uranium in uranyl compounds with extended structures,[33] this feature is also present in $UO_2(IO_3)_2(H_2O)$.[8] The U−O bond distance for the water in **1** is 2.450(7) Å, which is in the upper realm of U−O bond lengths. Figure 2 shows the crystal packing of the anionic ribbons and the Rb^+ cations in **1**.

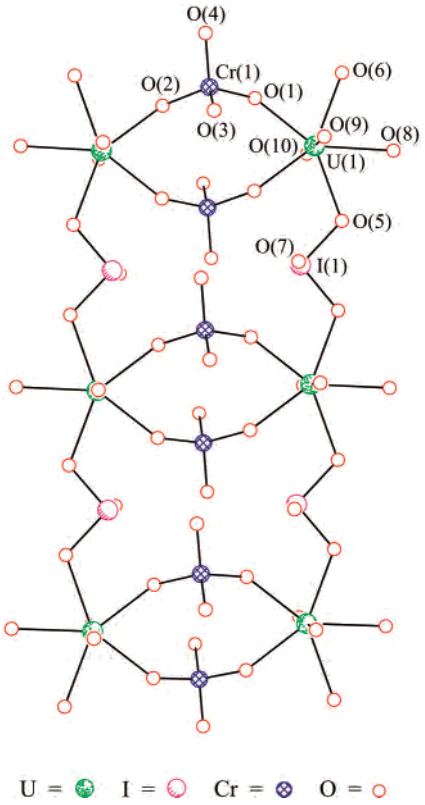

Figure 1. The one-dimensional, anionic $^1_\infty[UO_2(CrO_4)(IO_3)(H_2O)]^-$ ribbons in $Rb[UO_2(CrO_4)(IO_3)(H_2O)]$ (**1**).

The bond lengths for the $[CrO_4]$ tetrahedra and the iodate anions are within normal ranges, with a clear distinction displayed for bridging versus terminal Cr−O and I−O bond lengths. The two bridging oxygens bound to the iodine center have I−O bond lengths of 1.841(7) and 1.847(7) Å, and the one terminal I−O bond length is 1.785(7) Å. For the chromate anion, the two terminal oxygen atoms have Cr−O distances of 1.595(8) and 1.613(7) Å and the bridging oxygens have Cr−O bond lengths of 1.718(7) and 1.730(7) Å. One crystallographically unique Rb^+ cation balances charge in compound **1**. It forms eight long ionic contacts with oxygen atoms and resides in a distorted dodecahedral environment. A more detailed listing of bond distances and angles is given in Table 2. Bond valence sum calculations

(47) Hector, A. L.; Henderson, S. J.; Levason, W.; Webster, M. *Z. Anorg. Allg. Chem.* **2002**, *628*, 198.
(48) Sykora, R. E.; Albrecht-Schmitt, T. E. *Inorg. Chem.*, manuscript in preparation.

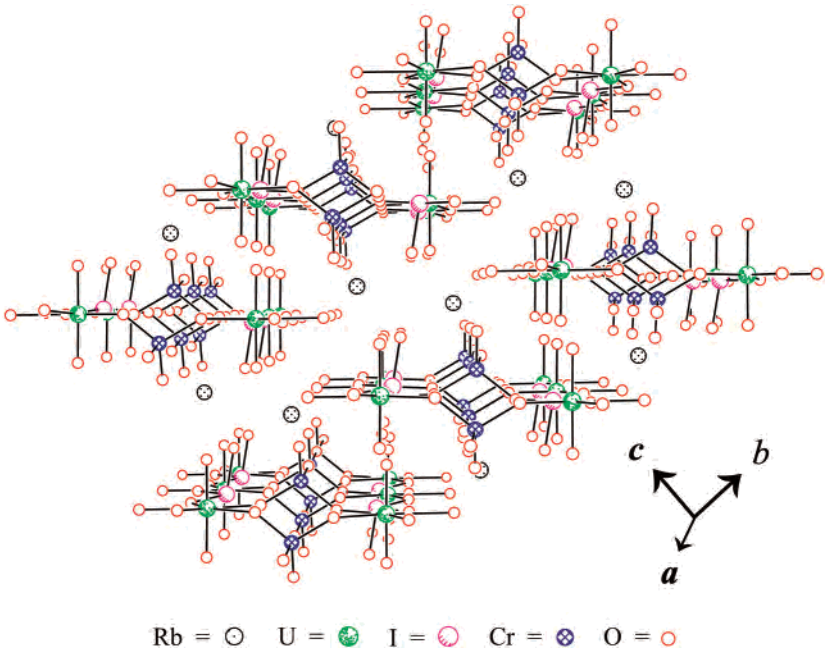

Figure 2. The packing of the $^{1}_{\infty}[UO_2(CrO_4)(IO_3)(H_2O)]^{-}$ ribbons in $Rb[UO_2(CrO_4)(IO_3)(H_2O)]$ (**1**).

Table 2. Selected Bond Distances (Å) and Angles (deg) for $Rb[UO_2(CrO_4)(IO_3)(H_2O)]$ (**1**)

Bond Lengths (Å)			
U(1)−O(1)	2.341(7)	Cr(1)−O(1)	1.730(7)
U(1)−O(2)′	2.314(7)	Cr(1)−O(2)	1.718(8)
U(1)−O(5)	2.397(7)	Cr(1)−O(3)	1.613(7)
U(1)−O(6)′	2.449(7)	Cr(1)−O(4)	1.595(8)
U(1)−O(8)	2.450(7)	I(1)═O(5)	1.847(7)
U(1)≡O(9)	1.767(7)	I(1)═O(6)	1.841(7)
U(1)≡O(10)	1.777(7)	I(1)═O(7)	1.785(7)
Angles (deg)			
O(9)−U(1)−O(10)	178.7(3)	O(2)−Cr(1)−O(4)	109.6(3)
O(1)−Cr(1)−O(2)	109.8(3)	O(3)−Cr(1)−O(4)	107.9(4)
O(1)−Cr(1)−O(3)	111.3(4)	O(5)−I(1)−O(6)	97.3(3)
O(1)−Cr(1)−O(4)	107.3(3)	O(5)−I(1)−O(7)	100.1(3)
O(2)−Cr(1)−O(3)	110.8(4)	O(6)−I(1)−O(7)	98.1(3)

Table 3. Bond Valence Sum Values for $Rb[UO_2(CrO_4)(IO_3)(H_2O)]$ (**1**), $K_2[UO_2(CrO_4)(IO_3)_2]$ (**2**), $Rb_2[UO_2(CrO_4)(IO_3)_2]$ (**3**), $Cs_2[UO_2(CrO_4)(IO_3)_2]$ (**4**), and $K_2[UO_2(MoO_4)(IO_3)_2]$ (**5**)

compd	$U^{VI}(1)$	$M^{VI}(1)$	$I^{V}(1)$	$I^{V}(2)$
1	5.98	5.76 (Cr)	4.85	
2	5.97	5.89 (Cr)	5.08	5.25
3	5.97	5.92 (Cr)	5.00	5.18
4	6.02	6.03 (Cr)	4.91	5.05
5	5.96	5.87 (Mo)	5.02	5.11

were performed on the U(VI), Cr(VI), and I(V) centers in **1**, and values are given in Table 3.[49−51]

$K_2[UO_2(CrO_4)(IO_3)_2]$ (2), $Rb_2[UO_2(CrO_4)(IO_3)_2]$ (3), $Cs_2[UO_2(CrO_4)(IO_3)_2]$ (4), and $K_2[UO_2(MoO_4)(IO_3)_2]$ (5). $K_2[UO_2(CrO_4)(IO_3)_2]$ (**2**), $Rb_2[UO_2(CrO_4)(IO_3)_2]$ (**3**), and $K_2[UO_2(MoO_4)(IO_3)_2]$ (**5**) are isostructural, and while $Cs_2[UO_2(CrO_4)(IO_3)_2]$ (**4**) crystallizes into a different space group, one-dimensional ribbons of the same type are contained in all four structures. Therefore, for the sake of brevity, the structures will be discussed simultaneously and differences

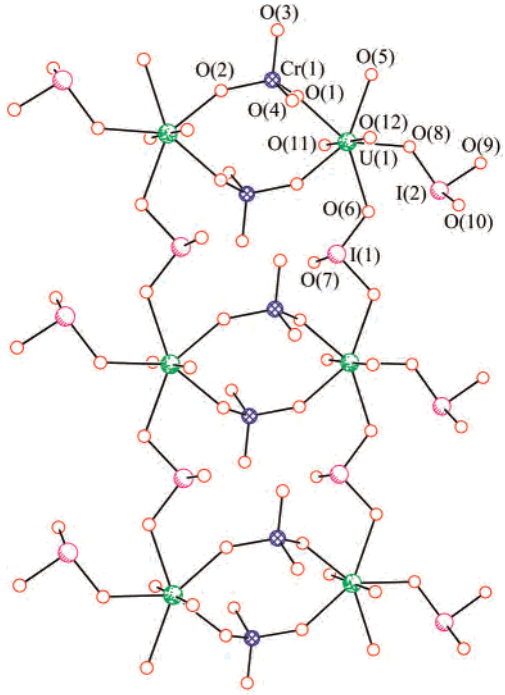

Figure 3. The one-dimensional, anionic $^{1}_{\infty}[UO_2(MO_4)(IO_3)_2]^{2-}$ ribbons found in $A_2[UO_2(MO_4)(IO_3)_2]$ (A = K, M = Cr (**2**); A = Rb, M = Cr (**3**); A = Cs, M = Cr (**4**); A = K, M = Mo (**5**)).

in the structures will be pointed out where appropriate. Compounds **2**−**5** all contain one-dimensional anionic $^{1}_{\infty}[UO_2(MO_4)(IO_3)_2]^{2-}$ (M = Cr (**2**−**4**), Mo (**5**)) ribbons (Figure 3). The ribbons of **2**−**5** are very similar to the $^{1}_{\infty}[UO_2(CrO_4)(IO_3)(H_2O)]^{-}$ ribbons of **1**. The main difference is that the coordinated water molecule in **1** is replaced with a terminal iodate group in compounds **2**−**5**, leading to a higher anionic charge and a wider ribbon. In **2**, **3**, and **5**,

(49) Brown, I. D.; Altermatt, D. *Acta Crystallogr.* **1985**, *B41*, 244.
(50) Brese, N. E.; O'Keeffe, M. *Acta Crystallogr.* **1991**, *B47*, 192.
(51) Burns, P. C.; Ewing, R. C.; Hawthorne, F. C. *Can. Mineral.* **1997**, *35*, 1551.

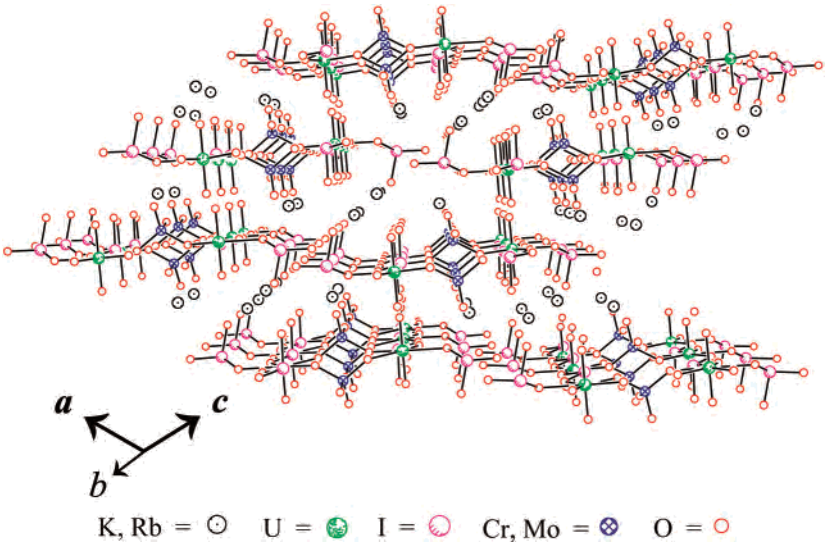

Figure 4. The parallel packing of the ribbons in the isostructural compounds $A_2[UO_2(MO_4)(IO_3)_2]$ (A = K, M = Cr (**2**); A = Rb, M = Cr (**3**); A = K, M = Mo (**5**)).

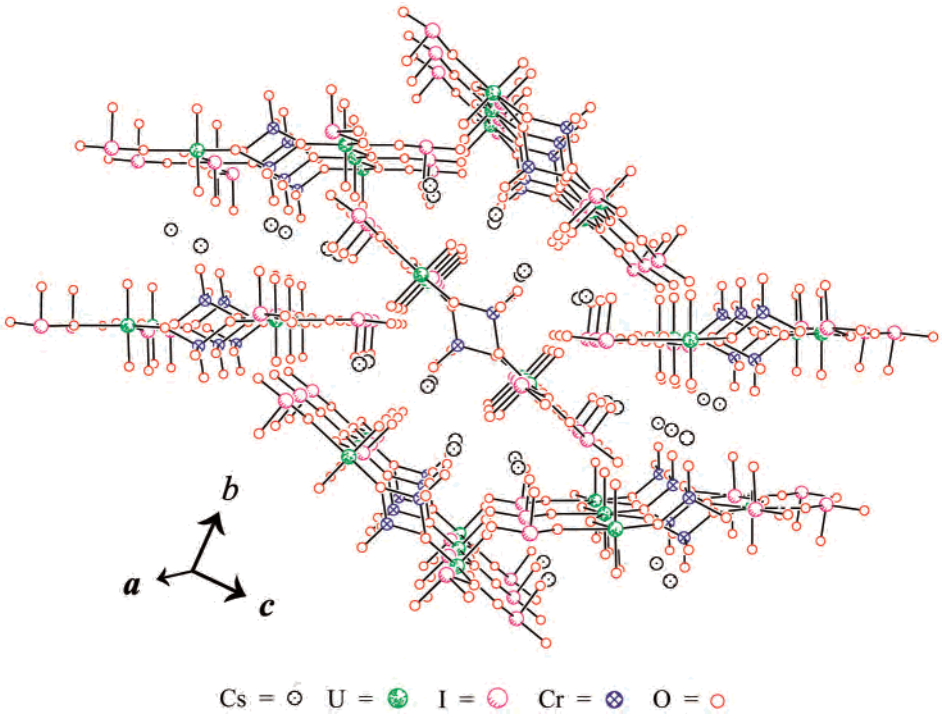

Figure 5. The packing of the ribbons in $Cs_2[UO_2(CrO_4)(IO_3)_2]$ (**4**). In **4**, half of the ribbons are rotated 47.4° in relation to the other ribbons.

the ribbons run along the *b*-axis, while in **4** the ribbons progress along the *a*-axis. K^+, Rb^+, or Cs^+ cations separate the ribbons and also serve to balance charge in the compounds. [UO_7] pentagonal bipyramids, bridging [MO_4] (M = Cr, Mo) tetrahedra, and both bridging and terminal iodate anions combine to form the anionic ribbons in **2**−**5**. The ribbons in **2**−**5** are terminated by monodentate iodate anions. This same type of chain termination is responsible for the one-dimensional structures of $K_2[(UO_2)_3(IO_3)_4O_2]$ and $Ba[(UO_2)_2(IO_3)_2O_2](H_2O)$ as well.[11,36]

The packing arrangement of the ribbons in **2**, **3**, and **5** varies from that observed for the Cs-containing structure. In compounds **2**, **3**, and **5** the ribbons pack parallel to one another as illustrated by Figure 4. Each structure contains two crystallographically unique A^+ cations holding the chains together through long ionic interactions ranging from 2.677-(6) to 3.494(4) Å. However, as shown by Figure 5, half of the ribbons in **4** are rotated around the *a*-axis by 47.4° in relation to the remaining half of the ribbons. In **4**, there are also two independent Cs^+ cations that serve to balance charge and knit the chains together with long ionic contacts to oxygen atoms ranging from 2.923(5) to 3.477(5) Å.

Each U(VI) center in **2**−**5** contains two U≡O bonds, with an average length of 1.783 Å and an average O≡U≡O bond angle of 179.1° for **2**−**5**, inclusively. The other five oxygen atoms coordinated to each U(VI) have distances ranging from 2.312(4) to 2.453(4) Å for the four compounds. Cr−O, Mo−O, and I−O bonds show standard variation based on whether

Table 4. Selected Bond Distances (Å) and Angles (deg) for $K_2[UO_2(CrO_4)(IO_3)_2]$ (**2**)

Bond Lengths (Å)			
U(1)−O(1)	2.331(6)	Cr(1)−O(3)	1.596(6)
U(1)−O(2)′	2.344(6)	Cr(1)−O(4)	1.609(6)
U(1)−O(5)	2.417(5)	I(1)═O(5)	1.815(6)
U(1)−O(6)′	2.405(5)	I(1)═O(6)	1.827(5)
U(1)−O(8)	2.351(6)	I(1)═O(7)	1.776(6)
U(1)≡O(11)	1.784(6)	I(2)═O(8)	1.835(5)
U(1)≡O(12)	1.792(5)	I(2)═O(9)	1.777(6)
Cr(1)−O(1)	1.713(6)	I(2)═O(10)	1.771(6)
Cr(1)−O(2)	1.702(6)		

Angles (deg)			
O(11)−U(1)−O(12)	179.3(3)	O(5)−I(1)−O(6)	98.6(3)
O(1)−Cr(1)−O(2)	109.9(3)	O(5)−I(1)−O(7)	97.5(3)
O(1)−Cr(1)−O(3)	107.7(3)	O(6)−I(1)−O(7)	98.6(3)
O(1)−Cr(1)−O(4)	111.4(3)	O(8)−I(2)−O(9)	98.4(3)
O(2)−Cr(1)−O(3)	108.4(3)	O(8)−I(2)−O(10)	99.5(3)
O(2)−Cr(1)−O(4)	110.1(3)	O(9)−I(1)−O(10)	99.3(3)
O(3)−Cr(1)−O(4)	109.3(3)		

Table 5. Selected Bond Distances (Å) and Angles (deg) for $Cs_2[UO_2(CrO_4)(IO_3)_2]$ (**4**)

Bond Distances (Å)			
U(1)−O(1)	2.312(4)	Cr(1)−O(3)	1.588(4)
U(1)−O(2)′	2.313(4)	Cr(1)−O(4)	1.604(4)
U(1)−O(5)	2.447(4)	I(1)═O(5)	1.839(4)
U(1)−O(6)′	2.453(4)	I(1)═O(6)	1.835(4)
U(1)−O(8)	2.315(4)	I(1)═O(7)	1.781(4)
U(1)≡O(11)	1.776(4)	I(2)═O(8)	1.843(4)
U(1)≡O(12)	1.789(4)	I(2)═O(9)	1.792(4)
Cr(1)−O(1)	1.702(4)	I(2)═O(10)	1.790(4)
Cr(1)−O(2)	1.687(4)		

Angles (deg)			
O(11)−U(1)-O(12)	178.5(2)	O(5)−I(1)−O(6)	99.9(2)
O(1)−Cr(1)−O(2)	110.4(2)	O(5)−I(1)−O(7)	97.9(2)
O(1)−Cr(1)−O(3)	107.3(2)	O(6)−I(1)−O(7)	99.0(2)
O(1)−Cr(1)−O(4)	111.3(2)	O(8)−I(2)−O(9)	95.2(2)
O(2)−Cr(1)−O(3)	107.7(2)	O(8)−I(2)−O(10)	102.6(2)
O(2)−Cr(1)−O(4)	110.9(2)	O(9)−I(2)−O(10)	99.9(2)
O(3)−Cr(1)−O(4)	109.0(3)		

the oxygen atoms are terminal or bridging. Cr−O and Mo−O bonds are typically 0.1 Å longer if the oxygen atom involved is bridging rather than terminally bound, while the average of the I−O bond lengths for the bridging oxygen atoms is only 0.05 Å greater than for the average I−O bond length for terminal oxygen atoms in **2**−**5**. Table 4 supplies a listing of selected bond lengths and angles for **2**, which are representative of bond lengths and angles for **3**. Bond lengths and angles for **4** and **5** are given in Tables 5 and 6, respectively. A comprehensive listing of bond lengths and angles for all compounds can be found in the Supporting Information. Bond valence sum calculations were performed on the U(VI), M(VI), and I(V) centers for **2**−**5**.[49−51] These values correlate well with expected results of VI, VI, and V, respectively, and are listed in Table 3.

Table 6. Selected Bond Distances (Å) and Angles (deg) for $K_2[UO_2(MoO_4)(IO_3)_2]$ (**5**)

Bond Distances (Å)			
U(1)−O(1)	2.351(2)	Mo(1)−O(3)	1.716(3)
U(1)−O(2)′	2.348(3)	Mo(1)−O(4)	1.728(3)
U(1)−O(5)	2.412(2)	I(1)═O(5)	1.825(2)
U(1)−O(6)′	2.412(2)	I(1)═O(6)	1.823(2)
U(1)−O(8)	2.366(3)	I(1)═O(7)	1.783(3)
U(1)≡O(11)	1.779(3)	I(2)═O(8)	1.831(2)
U(1)≡O(12)	1.785(3)	I(2)═O(9)	1.796(3)
Mo(1)−O(1)	1.820(3)	I(2)═O(10)	1.783(3)
Mo(1)−O(2)	1.809(3)		

Angles (deg)			
O(11)−U(1)−O(12)	179.4(1)	O(5)−I(1)−O(6)	98.9(1)
O(1)−Mo(1)−O(2)	110.8(1)	O(5)−I(1)−O(7)	98.6(1)
O(1)−Mo(1)−O(3)	108.8(1)	O(6)−I(1)−O(7)	99.2(1)
O(1)−Mo(1)−O(4)	111.3(1)	O(8)−I(2)−O(9)	98.6(1)
O(2)−Mo(1)−O(3)	108.7(1)	O(8)−I(2)−O(10)	99.1(1)
O(2)−Mo(1)−O(4)	108.7(1)	O(9)−I(2)−O(10)	99.9(1)
O(3)−Mo(1)−O(4)	108.5(1)		

Thermal Analysis. The thermal behavior of $Rb[UO_2(CrO_4)(IO_3)(H_2O)]$ (**1**) was evaluated using differential scanning calorimetry (DSC). These measurements were used to determine the dehydration temperature of **1**. A DSC thermogram for **1** was collected over a temperature range of 25−400 °C. A peak at 335 °C containing a shoulder at 329 °C was observed that likely corresponds to the loss of water from the compound. This is similar to the value of 327 °C obtained for the loss of a coordinated water in $UO_2(IO_3)_2(H_2O)$.[8]

Conclusions

Two new structure types based on a common ribbon have been discovered and structurally and spectroscopically characterized. The one-dimensional $^1_\infty[UO_2(MO_4)(IO_3)_2]^{2-}$ ribbons in **2**−**5** differ from the similar $^1_\infty[UO_2(CrO_4)(IO_3)(H_2O)]^-$ ribbons in **1** by the substitution of a terminal iodate anion for the coordinated water molecule in **1**. All five compounds discussed herein supply more examples of low-dimensional U(VI) structures containing C_{3v} anions. Ongoing investigations are probing the lability of the coordinated water molecule in **1**.

Acknowledgment. NASA (ASGC) and the Department of Energy, Heavy Elements Program (Grant No. DE-FG02-01ER15187), provided full support for the work described herein.

Supporting Information Available: ORTEP representations and X-ray crystallographic files in CIF format for $Rb[UO_2(CrO_4)(IO_3)(H_2O)]$ (**1**), $K_2[UO_2(CrO_4)(IO_3)_2]$ (**2**), $Rb_2[UO_2(CrO_4)(IO_3)_2]$ (**3**), $Cs_2[UO_2(CrO_4)(IO_3)_2]$ (**4**), and $K_2[UO_2(MoO_4)(IO_3)_2]$ (**5**). This material is available free of charge via the Internet at http://pubs.acs.org.

IC025773Y